Electronic Supplementary Information (ESI)

Atomic-Layer-Deposited SnO_2 on Pt/C Prevents Sintering of Pt Nanoparticles and Affects Reaction Chemistry for Electrocatalytic Glycerol Oxidation Reaction

Daewon Lee,‡[a] Youngmin Kim,[a] Hyunsu Han,[b] Won Bae Kim,[b] Hyunju Chang,[c] Taek-Mo Chung,[d] Jeong Hwan Han,[de] Hyun Woo Kim,*[c] Hyung Ju Kim*[af]*

[a] Chemical & Process Technology Division, Korea Research Institute of Chemical Technology (KRICT), 141 Gajeong-ro, Yuseong-gu, Daejeon 34114, South Korea. E-mail: hjkim@krict.re.kr

[b] Department of Chemical Engineering, Pohang University of Science and Technology (POSTECH), 77 Cheongam-Ro, Nam-gu, Pohang-si, Gyeongsangbuk-do 37673, South Korea.

[c] Chemical Data-Driven Research Center, Korea Research Institute of Chemical Technology (KRICT), 141 Gajeong-ro, Yuseong-gu, Daejeon 34114, South Korea. E-mail: ahwk@krict.re.kr

[d] Advanced Materials Division, Korea Research Institute of Chemical Technology (KRICT), 141 Gajeong-ro, Yuseong-gu, Daejeon 34114, South Korea.

[e] Department of Materials Science and Engineering, Seoul National University of Science and Technology, 232 Gongneung-ro, Nowon-gu, Seoul 01811, South Korea. E-mail: jhan@seoultech.ac.kr

[f] Advanced Materials and Chemical Engineering, University of Science and Technology (UST), 217 Gajeong-ro, Yuseong-gu, Daejeon 34113, South Korea.

‡ Present address: University of California at Berkeley and Lawrence Berkeley National Laboratory, Berkeley, CA 94720, United States

Supplementary Figures

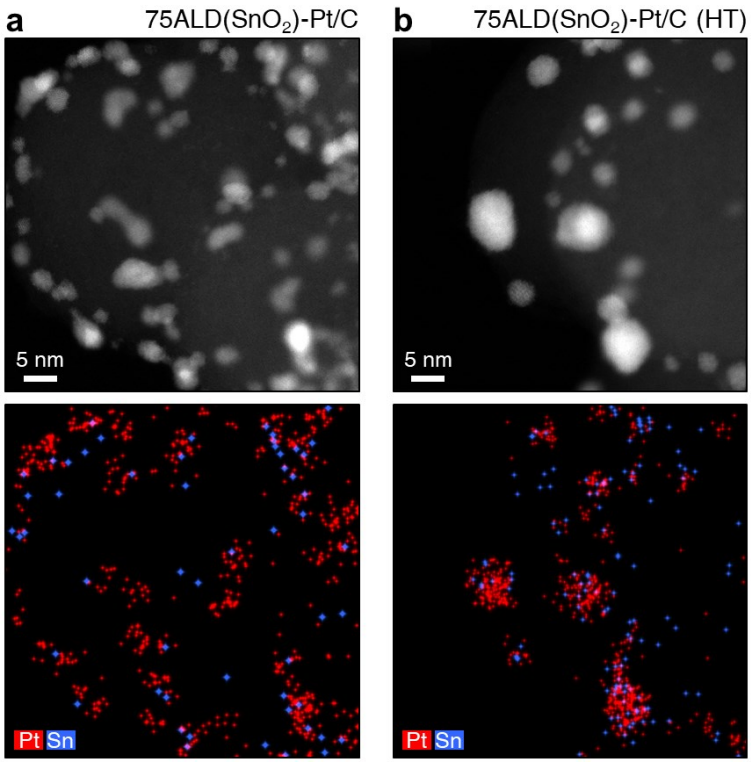

Fig. S1. Electron microscopy analysis of 75ALD(SnO_2)-Pt/C. a,**b**, HAADF-STEM images (upper) and corresponding EDS elemental mapping (lower) of the composite of Pt and Sn for 75ALD(SnO_2)-Pt/C (**a**) and 75ALD(SnO_2)-Pt/C (HT) (**b**).

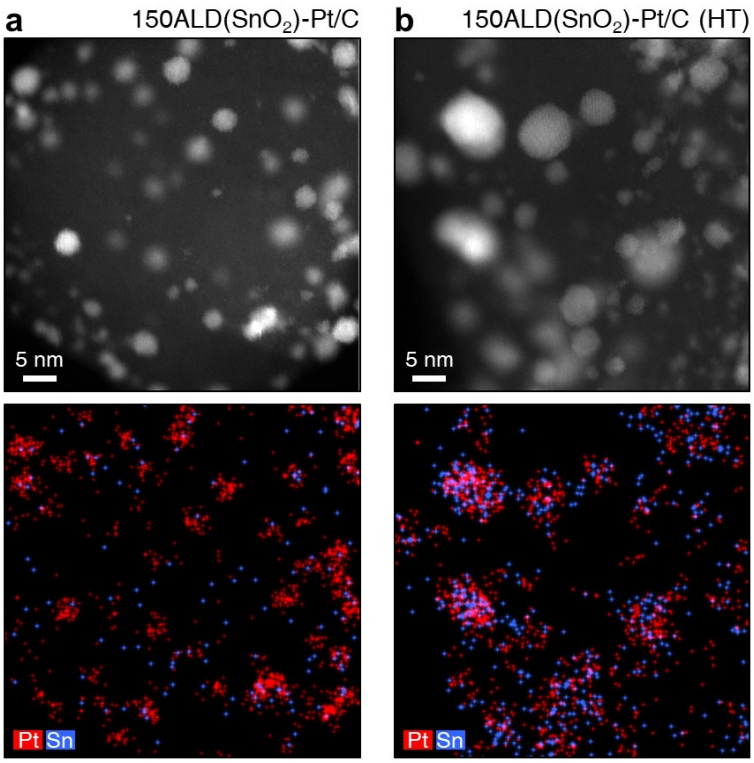

Fig. S2. Electron microscopy analysis of 150ALD(SnO_2)-Pt/C. a,**b**, HAADF-STEM images (upper) and corresponding EDS elemental mapping (lower) of the composite of Pt and Sn for 150ALD(SnO_2)-Pt/C (**a**) and 150ALD(SnO_2)-Pt/C (HT) (**b**).

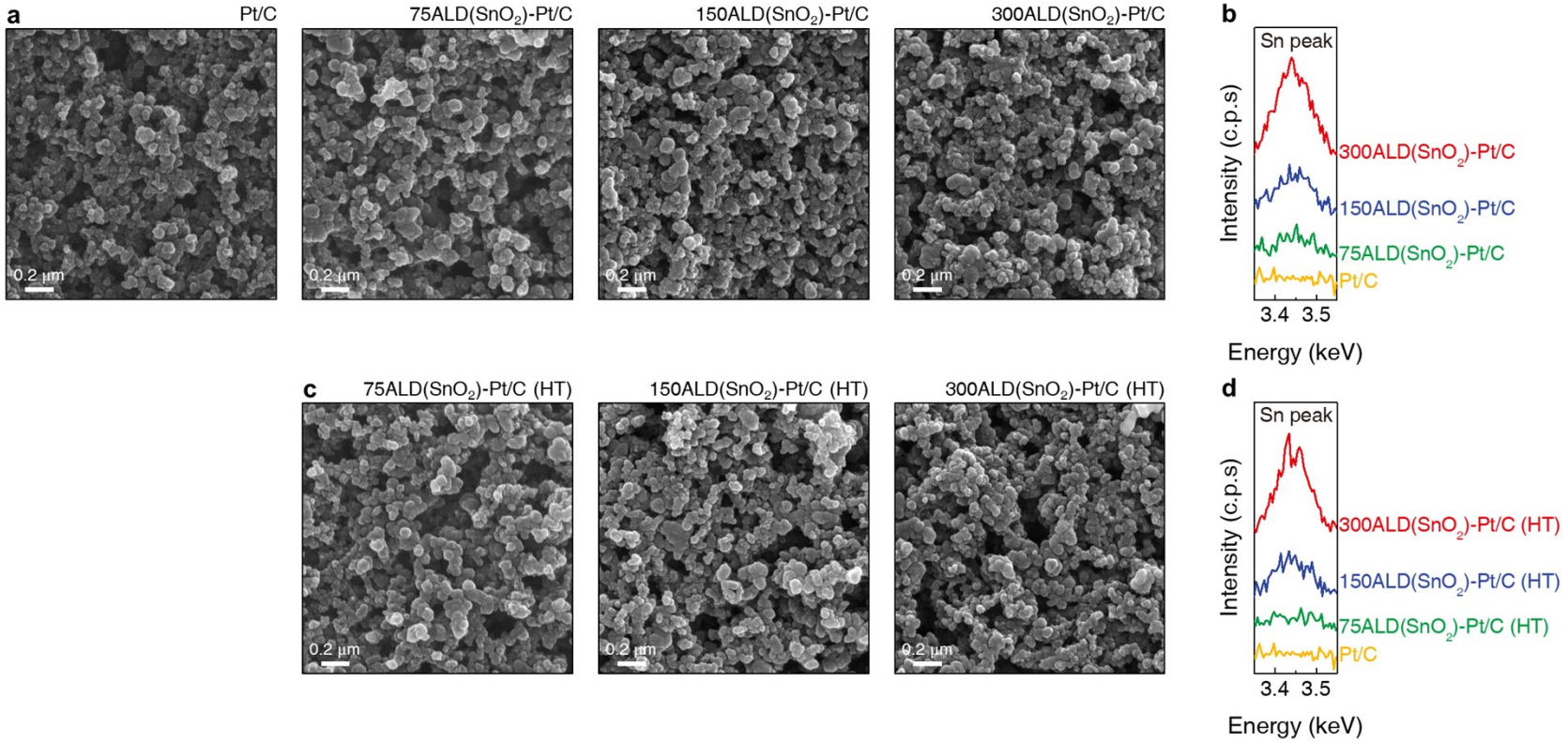

Fig. S3. Electron microscopy and elemental analyses of Pt/C and ALD(SnO_2)-Pt/C. a,**c**, SEM images for pristine Pt/C and ALD(SnO_2)-Pt/C with various ALD cycles before (**a**) and after (**c**) heat treatment. **b**,**d**, Corresponding EDS spectra demonstrating the existence of Sn for pristine Pt/C and ALD(SnO_2)-Pt/C with various ALD cycles before (**b**) and after (**d**) heat treatment.

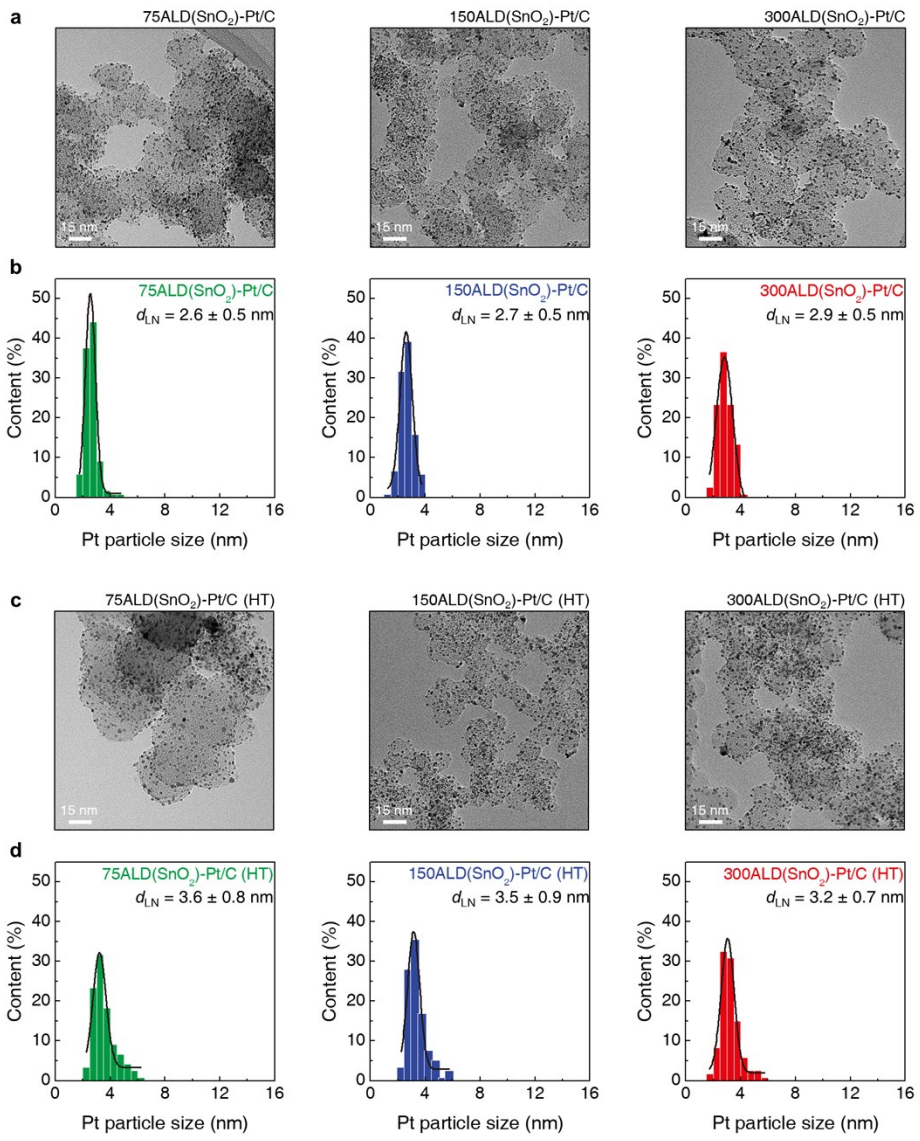

Fig. S4. Morphological, particle size, and particle size distribution analyses of ALD(SnO_2)-Pt/C before and after heat treatment. a,**b**,**c**,**d**, TEM images (**a**,**c**) and corresponding Pt particle size distribution (**b**,**d**) for ALD(SnO_2)-Pt/C with various ALD cycles before (**a**,**b**) and after (**c**,**d**) heat treatment. Note that estimated Pt particle length-number mean diameter (d_{LN}) values are presented for each specimen.

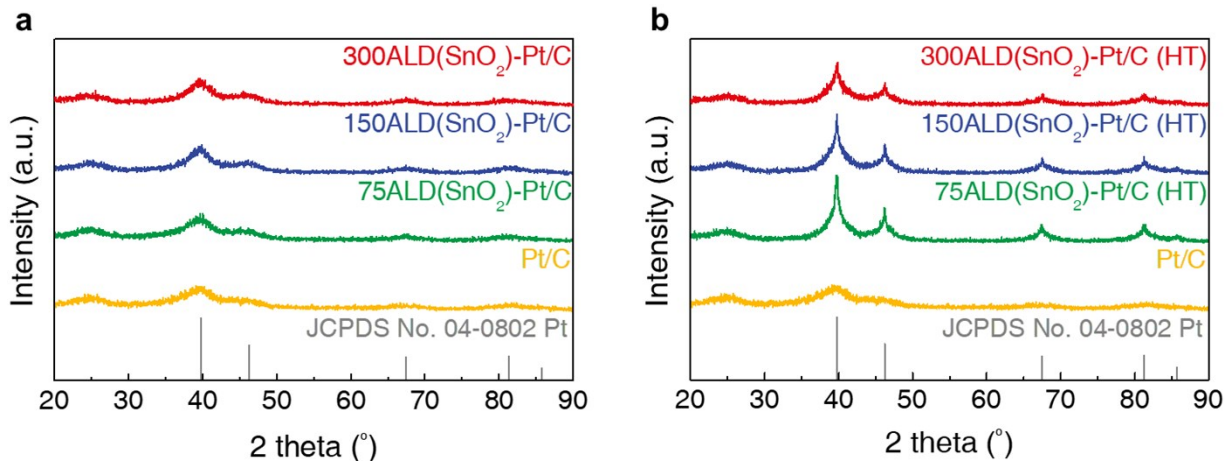

Fig. S5. XRD characteristics of Pt/C and ALD(SnO_2)-Pt/C. a,**b**, XRD spectra for pristine Pt/C and ALD(SnO_2)-Pt/C with various ALD cycles before (**a**) and after (**b**) heat treatment. For comparison, the reference crystallographic data for Pt (JCPDS No. 04-0802) are displayed.

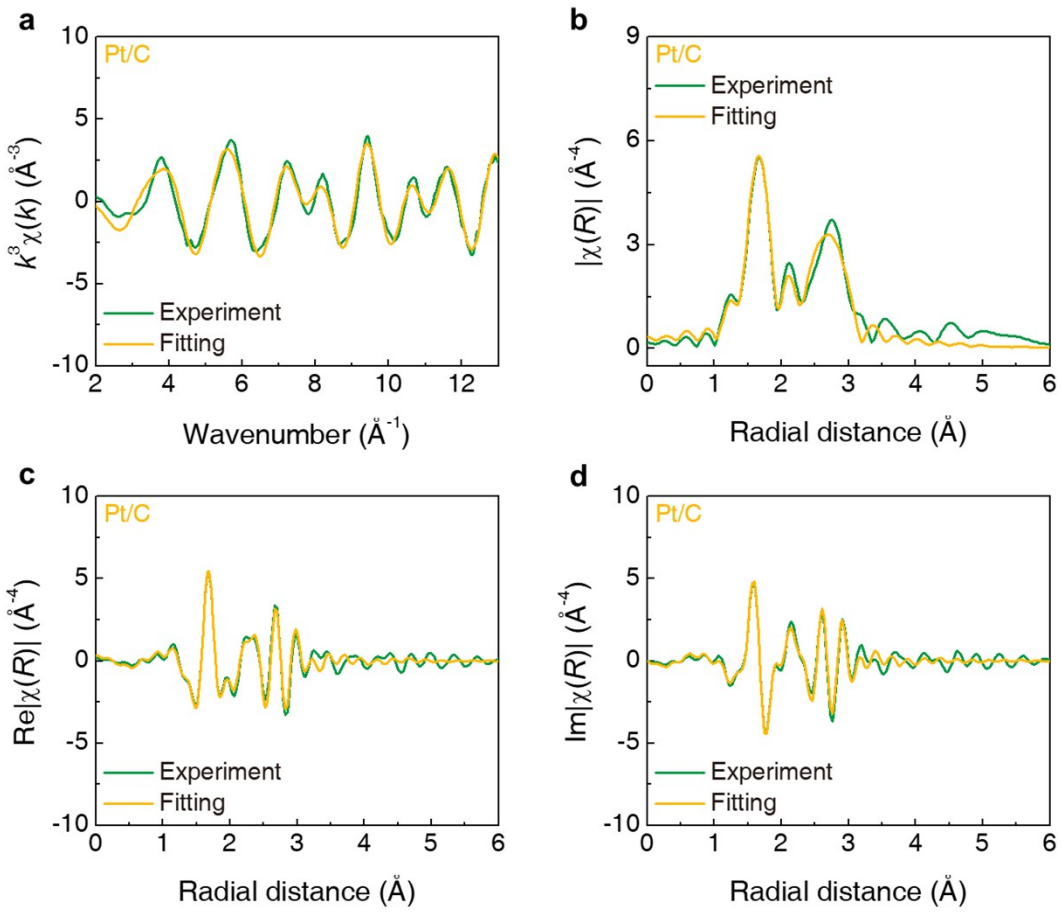

Fig. S6. Pt L_3-edge EXAFS fitting for Pt/C. a,**b**,**c**,**d**, k^3-weighted EXAFS function (**a**), the magnitude of k^3-weighted FT-EXAFS spectrum (**b**), and the real (**c**) and imaginary (**d**) parts of corresponding k^3-weighted FT-EXAFS spectrum from Pt L_3-edge of pristine Pt/C.

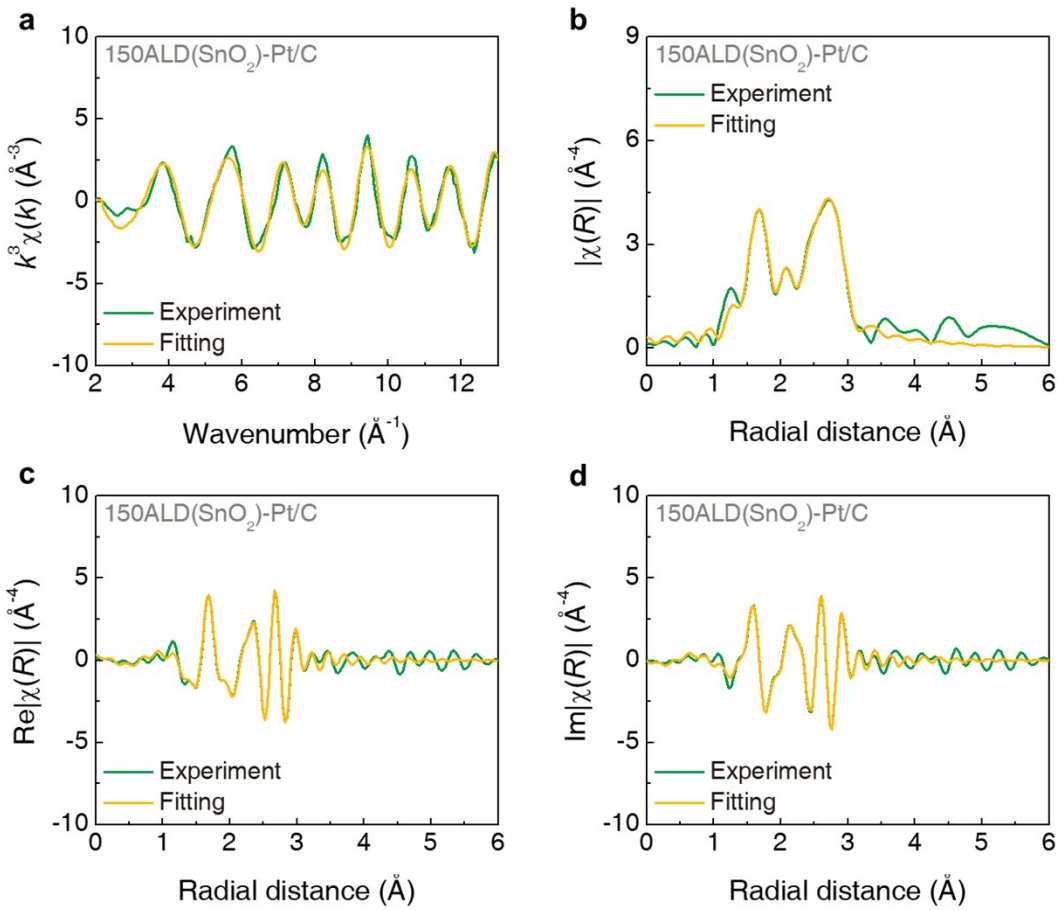

Fig. S7. Pt L_3-edge EXAFS fitting for 150ALD(SnO_2)-Pt/C. a,**b**,**c**,**d**, k^3-weighted EXAFS function (**a**), the magnitude of k^3-weighted FT-EXAFS spectrum (**b**), and the real (**c**) and imaginary (**d**) parts of corresponding k^3-weighted FT-EXAFS spectrum from Pt L_3-edge of 150ALD(SnO_2)-Pt/C.

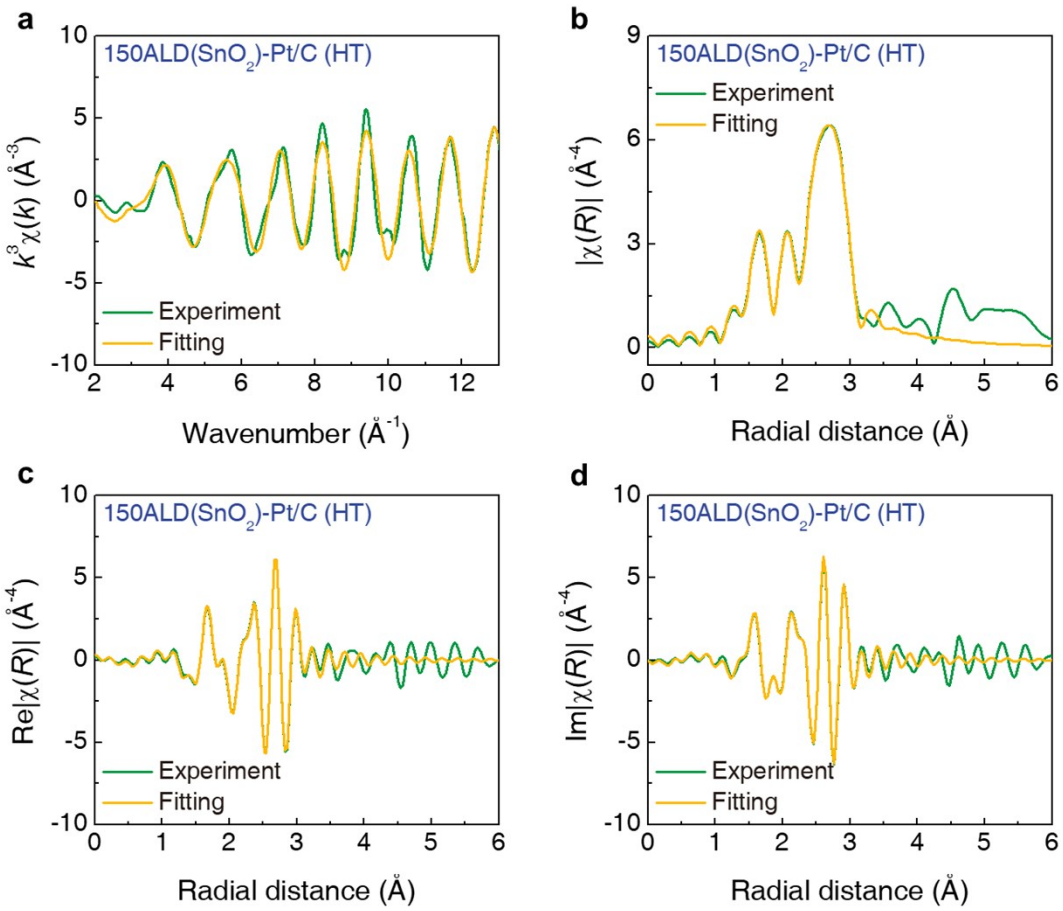

Fig. S8. Pt L_3-edge EXAFS fitting for 150ALD(SnO_2)-Pt/C (HT). a,**b**,**c**,**d**, k^3-weighted EXAFS function (**a**), the magnitude of k^3-weighted FT-EXAFS spectrum (**b**), and the real (**c**) and imaginary (**d**) parts of corresponding k^3-weighted FT-EXAFS spectrum from Pt L_3-edge of 150ALD(SnO_2)-Pt/C (HT).

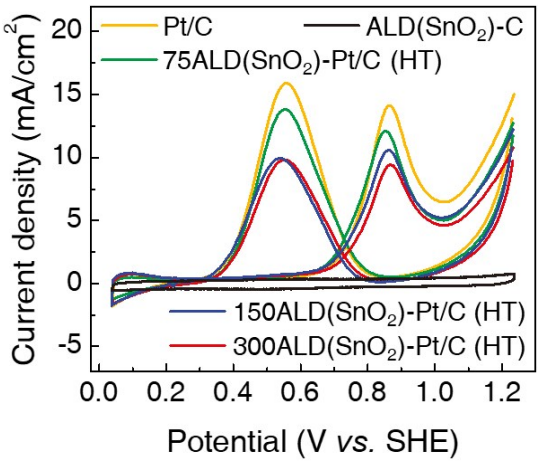

Fig. S9. Supplementary electrochemical performance analysis in an electrochemical half-cell system for Pt/C and heat-treated ALD(SnO_2)-Pt/C catalysts for the electrocatalytic GOR. CV curves corresponding to current density for the electrocatalytic GOR over pristine Pt/C and heat-treated ALD(SnO_2)-Pt/C with various ALD cycles in 2 M glycerol/0.5 M H_2SO_4 solution at room temperature.

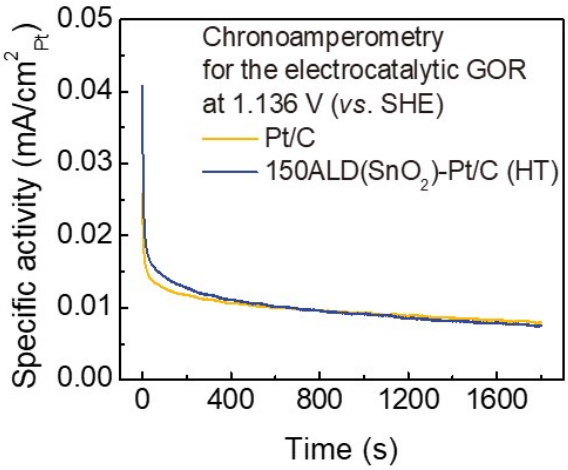

Fig. S10. Supplementary electrochemical performance analysis of Pt/C and heat-treated 150ALD(SnO_2)-Pt/C catalysts for the electrocatalytic GOR in an electrochemical batch reactor system. Chronoamperometry corresponding to specific activity for the electrocatalytic GOR over pristine Pt/C and 150ALD(SnO_2)-Pt/C (HT) catalysts.

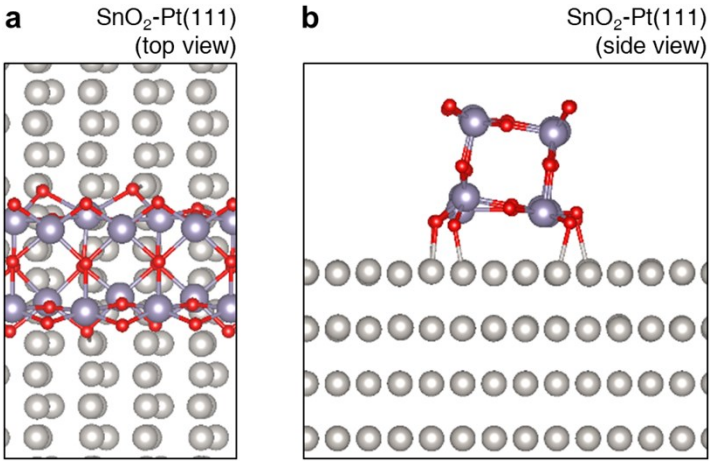

Fig. S11. Computational surface models. a,**b**, Optimized model of SnO_2-Pt(111) surface in top (**a**) and side (**b**) views. As the initial SnO_2 structure is extracted from the SnO_2(110) surface, the optimized SnO_2 structure shows characteristics of the SnO_2 (110) surface.

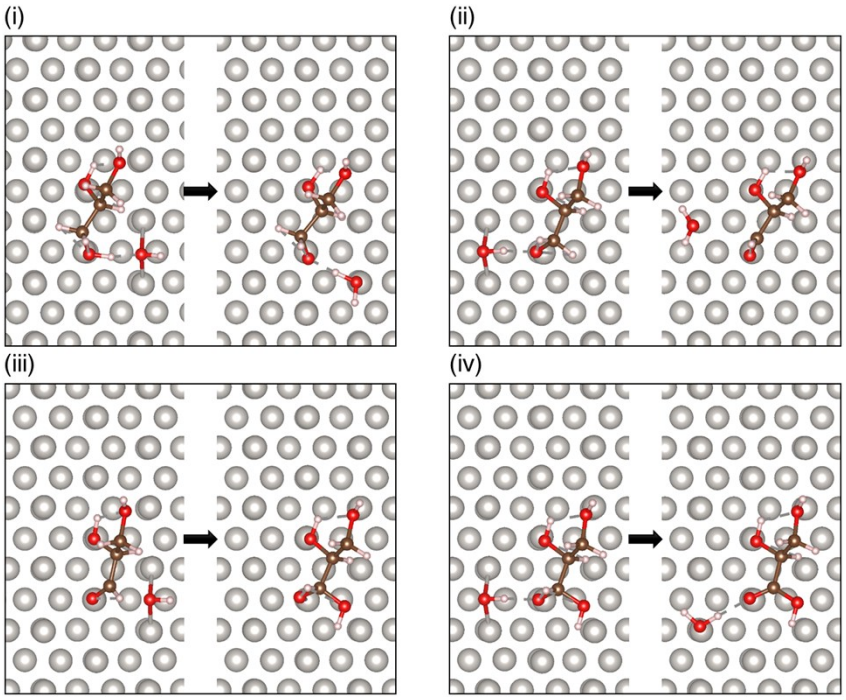

Fig. S12. Optimized atomistic structures (top view) of a possible reaction pathway for the electrocatalytic oxidation from glycerol to *GLA* via *GAD*, on the Pt(111) surface.

Supplementary Scheme

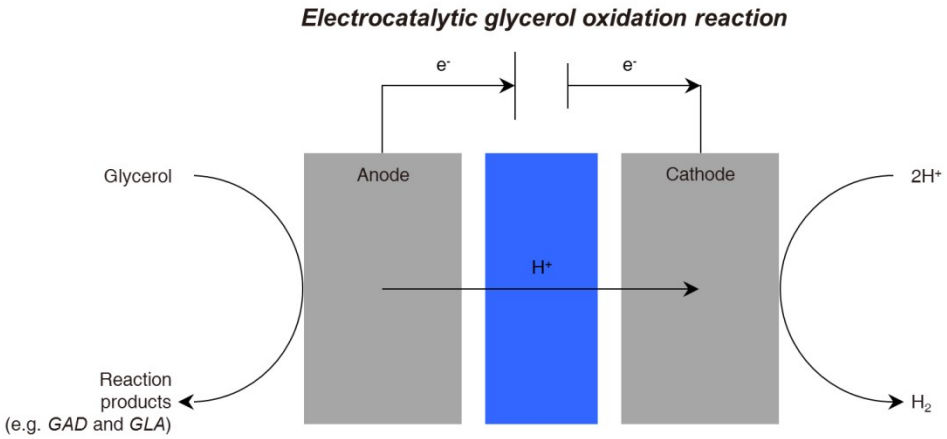

Scheme S1. Schematic illustration of an electrolysis cell system for electrocatalytic GOR technology to co-produce renewable chemicals and hydrogen.

Supplementary Tables

Table S1. Summary of the length-number mean diameter (d_{LN}) of Pt particles for ALD(SnO_2)-Pt/C with various ALD cycles before and after heat treatment. Note that the changes in d_{LN} after heat treatment are depicted.

	75ALD(SnO_2)-Pt/C	**150ALD(SnO_2)-Pt/C**	**300ALD(SnO_2)-Pt/C**
Before HT (nm)	2.6±0.5	2.7±0.5	2.9±0.5
After HT (nm)	3.6±0.8	3.5±0.9	3.2±0.7
Change (nm)	1.0	0.8	0.3

Table S2. Summary of the obtained electrochemical Pt surface area and Pt metal dispersion (D_{echem}) *via* H_2 desorption for pristine Pt/C and heat-treated ALD(SnO_2)-Pt/C with various ALD cycles.

	Pt/C	**75ALD(SnO_2)-Pt/C (HT)**	**150ALD(SnO_2)-Pt/C (HT)**	**300ALD(SnO_2)-Pt/C (HT)**
Electrochemical Pt surface area (cm^2)	2.55	1.98	2.04	2.20
Electrochemical Pt surface area per Pt loading (m^2/g_{Pt})	82.38	65.88	70.59	80.48
D_{echem}	0.33	0.26	0.28	0.32

Table S3. Comparison of the catalytic activity for electrocatalytic GOR with the reported Pt-based catalysts.

Catalyst	Reaction Solution	Scan Rate (mV/s)	Electrocatalytic GOR	Reference
			Specific Activity (mA/cm^2_{Pt})[a]	
PtNi/C	2 M glycerol + 0.5 M H_2SO_4	50	0.27	S1
Co@Pt/CCE	0.5 M glycerol + 0.5 M H_2SO_4	50	0.25	S2
PtAu@Ag	1 M glycerol + 0.1 M $HClO_4$	10	0.27	S3
Pt nanoflowers	1 M glycerol + 0.5 M H_2SO_4	50	0.32	S4
75ALD(SnO_2)-Pt/C (HT)	2 M glycerol + 0.5 M H_2SO_4	50	0.43	This work

[a] *Current density normalized by the electrochemically active surface area. Some values were calculated by information given in the reference.*

Supplementary References

S1 S. Lee, H. J. Kim, S. M. Choi, M. H. Seo and W. B. Kim, *Appl. Catal., A*, 2012, **429-430**, 39-47.

S2 B. Habibi and S. Ghaderi, *Int. J. Hydrogen Energy*, 2015, **40**, 5115-5125.

S3 Y. Zhou, Y. Shen and J. Xi, *Appl. Catal., B*, 2019, **245**, 604-612.

S4 Y. Zuo, L. Wu, K. Cai, T. Li, W. Yin, D. Li, N. Li, J. Liu and H. Han, *ACS Appl. Mater. Interfaces*, 2015, **7**, 17725-17730.